

RXTE Spectrum of A2319

Duane Gruber¹, and Yoel Rephaeli^{1,2}

¹*Center for Astrophysics and Space Sciences, University of California, San Diego, La Jolla, CA 92093-0424*

²*School of Physics and Astronomy, Tel Aviv University, Tel Aviv, 69978, Israel*

ABSTRACT

The cluster of galaxies A2319 was observed in 1999 for ~ 160 ks by the PCA and HEXTE instruments aboard the RXTE satellite. No noticeable variability is seen in the emission measured by either instrument over the ~ 8 week observation. The quality of the data allows, for the first time, a meaningful search for emission whose spectral properties are distinct from those of the primary thermal emission with (previously measured) mean temperature in the range $8 - 10$ keV. Fitting the RXTE data by a single thermal component we obtain $kT = 8.6 \pm 0.1$ (all errors are 90% confidence limits), a low iron abundance $Z_{Fe} \sim 0.16 \pm 0.02$, and large positive residuals below 6 keV and between 15 to 30 keV. The quality of the fit is *drastically improved* if a second component is added. A two-temperature model yields $kT_1 \simeq 10.1 \pm 0.6$, $kT_2 \simeq 2.8 \pm 0.6$, and of $Z_{Fe} \sim 0.23 \pm 0.03$ which is consistent with previously measured values. An equally good fit is obtained by a combination of a primary thermal and a secondary nonthermal component, with $kT \simeq 8.9 \pm 0.6$, and power-law (photon) index $\alpha \simeq 2.4 \pm 0.3$. We have repeated the analysis by performing joint fits to both these RXTE measurements and archival ASCA data. At most 25% of the RXTE secondary component could be present in the ASCA data. Allowing for this difference, very similar results were obtained, with only somewhat different values for the temperature ($kT = 9.2 \pm 0.5$) and power-law index ($\alpha \simeq 2.5 \pm 0.3$) in the latter model. The deduced value of α is consistent with the measured spectrum of extended radio emission in A2319. Identifying the power-law emission as Compton scattering of the radio-emitting electrons by the CMB, we obtain $B \sim 0.1 - 0.3 \mu G$ for the volume-averaged magnetic field, and $\sim 4 \times 10^{-14} (R/2Mpc)^{-3}$ erg cm⁻³ for the mean energy density of the emitting electrons in the central region (radius R) of A2319.

Subject headings: Galaxies: clusters: general — galaxies: clusters: individual (A2319) — galaxies: magnetic fields — radiation mechanisms: non-thermal

1. Introduction

The main goals of current work on X-ray emission from clusters of galaxies are refined spectral and spatial mappings to determine density and temperature profiles of intracluster (IC) gas, its abundance gradients, and to search for additional spectral components. An isothermal gas distribution usually provides a good overall spectral fit to the continuum and (usually prominent) Fe K_α line, but some temperature variations have already been measured in a few clusters. This is not surprising, as the gas distribution over typical radial regions $\simeq 2$ Mpc is not expected to be fully isothermal.

In clusters with extended radio emission, there could also be an appreciable additional *non-thermal* X-ray emission, possibly from Compton scattering of the radio-emitting relativistic electrons by the Cosmic Microwave Background (CMB) radiation (Rephaeli 1979), or by nonthermal bremsstrahlung from a suprathermal electron population (Kaastra *et al.* 1998, Sarazin & Kempner 2000). Measurements of clusters at high X energies are therefore of considerable interest: Significant additional insight is expected on physical conditions in the IC plasma, including the strength of magnetic fields, density and energy spectra of relativistic or suprathermal electrons and protons, and the interaction of these particles with the gas (Rephaeli 1979, Rephaeli & Silk 1995). Search for emission at energies higher than 20 keV can be currently made only with the PDS and HEXTE instruments aboard BeppoSAX and RXTE, respectively.

Initial attempts to detect nonthermal emission from a few clusters with the HEAO-1, CGRO, ASCA, satellites were unsuccessful (Rephaeli, Gruber & Rothschild 1987, Rephaeli & Gruber 1988, Rephaeli, Ulmer & Gruber 1994, Henriksen 1998). The improved sensitivity and wide spectral range of the RXTE and BeppoSAX satellites have recently led to major progress in the

search for this emission. Clear evidence for the presence of a second component in the spectrum of the Coma cluster was seen in the analysis of RXTE observations (Rephaeli, Gruber, & Blanco 1999; hereafter RGB). While the detection of the second component was not significant at high energies (where it is predicted to dominate the emission), RGB have argued that this component is more likely to be nonthermal, rather than a second, low temperature component. Indeed, this nonthermal component was directly detected at energies 25 – 80 keV by BeppoSAX observations (Fusco-Femiano *et al.* 1999). Power-law components were also detected by BeppoSAX in two other clusters, A2199 (Kaastra *et al.* 2000), and A2256 (Fusco-Femiano *et al.* 2000); only upper limits were obtained from RXTE measurements of A2256 (Henriksen *et al.* 1999), and A754 (Valinia *et al.* 1999).

Emission from nonthermal electrons may also contribute at low energies, and there are claims that this emission has been measured. EUV observations of several clusters have reportedly led to the measurement of diffuse low-energy (65 – 245 eV) emission which is possibly nonthermal (Sarazin & Lieu 1998, Bowyer & Berghofer 1998). However, Bowyer *et al.* (1999) argue that this emission has been unequivocally detected *only* in the Coma cluster.

The above RXTE and BeppoSAX results provide strong motivation for extending the search for nonthermal components in cluster spectra. Here we present the results of ~ 160 ks RXTE observations of A2319, another cluster with extended radio emission region. The spectral analysis is based on these measurements, as well as archival data from a ~ 57 ks observation with the ASCA satellite.

2. Observations and Data Reduction

A2319 was observed by the Proportional Counter Array (PCA) and the High Energy X-ray Timing Experiment (HEXTE) on RXTE during 48

separate pointings totaling approximately 160 ks between 1999 December 3, and 2000 January 20. Spectra were accumulated by the PCA in ‘Standard 2’ mode, which results in a 129-channel count spectrum from 3 to 120 keV. The HEXTE, which consists of two independent clusters of detectors, returned data in event-by-event mode which were subsequently accumulated into 256-channel spectra spanning 18–250 keV. To subtract the background, each HEXTE cluster was commanded to beamswitch every 16 s between on-source and two alternate off-source positions 1.5° on either side.

Standard screening criteria were applied to the data segments (Earth elevation angle, spacecraft pointing, avoidance of the South Atlantic Anomaly), resulting in a net exposure time of 156992 s (as measured by the PCA, which has negligible dead time). PCA detectors 0 and 2 were on during all of this time; detectors 1, 3 and 4 were enabled only occasionally, and data from them was not used. After correcting for dead-time effects, the corresponding on-source live-times for the HEXTE were 61586 s and 61818 s for clusters A and B, respectively, with off-source live-times nearly equal to 87% of these values.

The PCA background was estimated with the ‘L7/240’ faint source model provided by the instrument team. The background model appears to be less successful at predicting the high energy (> 22 keV) counting rate than the models for observing rounds 1 – 3. The higher channels are under-predicted by an amount which increases with energy, reaching 2% at 120 keV. In the following section we explicitly treat the uncertainty resulting from errors of background prediction and show that it has a negligible effect on the conclusions of the analysis. The HEXTE background was determined from the off-source pointings, and showed no problems to a level of less than 1%.

3. Spectral Analysis

We have first carried out an exhaustive analysis of the above RXTE observations, and then performed a joint analysis of the RXTE data with 57 ks of public ASCA data. The 160 ks RXTE observation of A2319 provides a large and *uniform* dataset. The inclusion of ASCA measurements can potentially yield additional spectral insight, particularly in the energy range 0.8–3 keV, and some spatial information. This, however, comes at a price in the form of substantial additional systematics, such as the energy dependence of the point spread function (*e.g.*, Irwin, Bregman & Evrard 1999).

3.1. RXTE Data

For each PCA detector, the net counting rate on-source was about 14 count/s, compared to a background rate of 13 count/s; thus A2319 ($z = 0.056$) was easily detected. Since we could find no evidence for temporal variability in the PCA source and background rates over the observations, we used the time-integrated PCA and HEXTE spectra to form the basic data set for spectral analysis.

Response matrices were generated with standard tools, and a small allowance was applied for PCA systematic errors (see Wilms *et al.* 1999) in the amount of 0.4%. Additionally, PCA spectral channels below 3 keV and above 22 keV were excluded because of sensitivity to artifacts in the background model, and the small effective area of the PCA outside this range. The HEXTE data were restricted to the energy range 18–100 keV for similar reasons, resulting in source and background counting rates of 1.2 and 128 count/s respectively (cluster A), and 0.9 and 90 count/s (cluster B). We tested for errors arising from inaccurate PCA background estimation in several ways, and concluded that the spectral results obtained here are quite robust with respect to errors of background determination. With well-fitting two-component models, we found that the best-

fit model parameters changed negligibly when the PCA upper energy cut was extended from 22 to 60 keV. We also noted little change of these parameters when the background estimate was reduced by 1% for better subtraction above 30 keV; this was the case with either PCA energy cutoff. Finally, we investigated the effect of orbital data selection by including more data following passage of the satellite through the South Atlantic Anomaly region, with its high particle fluxes. Although only 5000 more seconds were collected, there was a dramatic increase by a factor of three of a barely noticeable spectral line at 16 keV. We thus feel that uncorrected PCA background is largely removed by the selection procedure, to a level which is adequately treated with the 0.4% systematic error allowance. After initial testing with full energy resolution, the observed spectra were rebinned such that the oversampling was reduced to 1.5 – 2 bins per energy resolution element, in order to sharpen comparison among trial spectral models in the final fitting. Data from the individual PCA detectors was combined into a single spectrum, and similarly a single HEXTE spectrum was prepared from the two clusters.

Most of the observed emission is clearly thermal, so we have first determined spectral parameters of a single isothermal gas component. The best-fit temperature (using either the MEKAL, or Raymond-Smith thermal emission models) in this case is 8.6 ± 0.1 keV, in moderate disagreement with the value 9.6 ± 0.3 keV determined from BeppoSAX (Molendi *et al.* 1999), and the value of 10.0 ± 0.7 keV from ASCA (Markevitch 1996) measurements. The observed Fe XXV K_α line yields an abundance $Z_{Fe} \simeq 0.16 \pm 0.02$ (in solar units), appreciably lower than the BeppoSAX and ASCA values, 0.25 ± 0.03 , and 0.30 ± 0.08 , respectively. No cold absorption was measurable, and given the 3 keV PCA threshold, none was expected. This best-fit model has an enormous χ^2 of 216 for 31 degrees of freedom. Concave upwards PCA residuals indicate that an extra com-

ponent is required. In particular, both PCA and HEXTE show strong positive residuals between 15 and 30 keV. When a second thermal component is added, we obtain the best-fit parameters (Table 1) which imply an appreciable fraction, $\sim 15\%$, for the (2 – 10 keV) flux in the second component. All errors are at the 90% confidence level, estimated by taking correlations between the various parameters into account (using the procedure of Lampton, Margon & Bowyer 1976) for the cases of two to four ‘interesting’ parameters.

Equally likely is a power-law fit for the second component, shown in Figure 1, with statistics $\Delta\chi^2 = 182$, $\chi^2=34$, and 29 dof. The need for two components is overwhelmingly significant, with the chance probability less than 10^{-10} . The best-fit photon index is 2.4 ± 0.3 , and the temperature of the thermal component is 8.9 ± 0.6 keV, not significantly different from the value for the single temperature fit. The deduced nonthermal 2–10 flux is $(4.0 \pm 1.0) \times 10^{-11}$ erg cm $^{-2}$ s $^{-1}$. With this power-law component, $Z_{Fe} \simeq 0.27 \pm 0.04$, in complete agreement with previously determined values. Figure 1 shows the fitted thermal and power-law components separately. The strong detection of a second component rests largely on the PCA spectrum from 3 to 6 keV. But the data *above 18 keV*, for which the fitted power-law flux is about equal that of the isothermal component, independently indicate a power-law second component. By fitting only HEXTE data above 18 keV with the isothermal parameters fixed at their values determined over the entire energy range, the power-law component has joint 90% confidence intervals of [0.6, 1.2] in units of 10^{-11} erg cm $^{-2}$ s $^{-1}$ for the 18–40 keV flux, and [1.8, 5.0] for the index. Both values are consistent with the globally-determined estimates. If the index is held fixed at 2.4, the power-law flux above 20 keV is significant at the 8σ level.

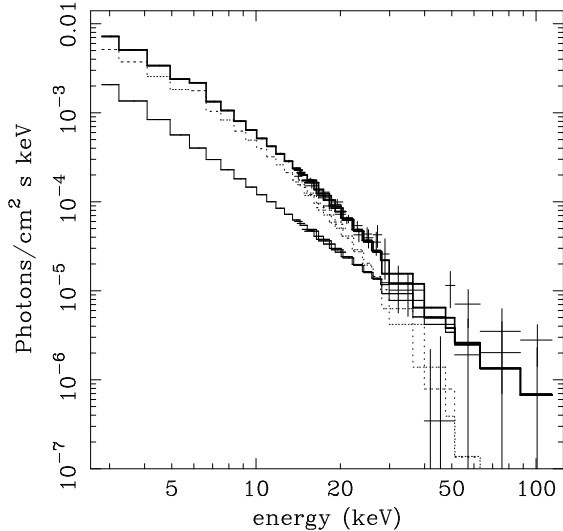


Fig. 1.— Unfolded RXTE data and combined Raymond-Smith plus power-law models with 8.9 ± 0.6 keV and index of 2.4 ± 0.3 , shown individually, as well as their sum.

3.2. Joint RXTE and ASCA Datasets

ASCA data provide a comfortable spectral overlap with RXTE data between 3 and 8 keV, so if the second component is not time variable, we can attempt to confirm it through joint fitting of both datasets. ASCA spectra were extracted using standard tools from the cleaned archival GIS event files. Extraction radii between 15 and 20 arcminutes were found to include essentially the whole cluster emission. We chose 0.8 – 8.0 keV as the most reliable band for ASCA spectra, and grouped the hundreds of energy channels in this range into 21 spectral bins, each of width $\delta E/E = 0.1$. Data from the two GIS detectors were also combined. As with the RXTE PCA, we added systematic noise of about 1% per final spectral bin.

Fitting a single Raymond-Smith spectral form to the ASCA data alone, we obtained a temperature of 12.5 keV, considerably higher than the 10 keV reported by Markevitch (1996). By narrowing the extraction radius to the 6 arcminutes that is used for point sources, we obtained a kT

of 9 keV, much more consistent with temperatures obtained by Markevitch (1996), BeppoSAX (Molendi *et al.* 1999), and here with RXTE. We then checked the spectral inter-calibration of ASCA and RXTE, as well as the standard analysis tools, on the Crab. With both ASCA and RXTE we obtained a spectral index of 2.08. Thus we were very confident of the on-axis effective area calibration of ASCA, but felt that the effective area at 5 – 15 arcminutes off-axis may be underestimated by about 10% at higher energies. Because of the exact agreement on the Crab, we employed the ASCA data extracted with 5 arcminute radius for the joint analysis with RXTE. With this radius a fraction 0.59 of the cluster flux is collected, so a normalization constant of 0.59 for the ASCA spectrum was initially used in the analysis. When allowed to float in the joint analysis, values near 0.6 are in fact obtained.

In the joint fits the main component was modeled as a Raymond-Smith plasma emission; a Mekal model produced nearly identical results in all fits. A fit with a single temperature had χ^2 of 313 for 50 degrees of freedom. The RXTE PCA data (see Figure 2, middle panel) were mainly responsible for this very poor fit. Two-temperature models produced negligible improvement in χ^2 . Likewise, a thermal plus power-law model produced little improvement in χ^2 . Thus, the ASCA data do not confirm the power-law or low-temperature thermal component so strongly indicated by the RXTE data alone. Nevertheless, when the condition of equal RXTE and ASCA intensity for the second component is relaxed, reduced χ^2 drops from the value 6 to near unity. In these best-fit models the flux of the secondary component is not significant in the ASCA data. Completely acceptable χ^2 values were achieved by fitting an additional power-law or thermal model to the RXTE data. With the inclusion of the ASCA data the best-fit parameters differ little from the RXTE-only fits, as shown in Table 1. The temperature and abundance of the primary component are

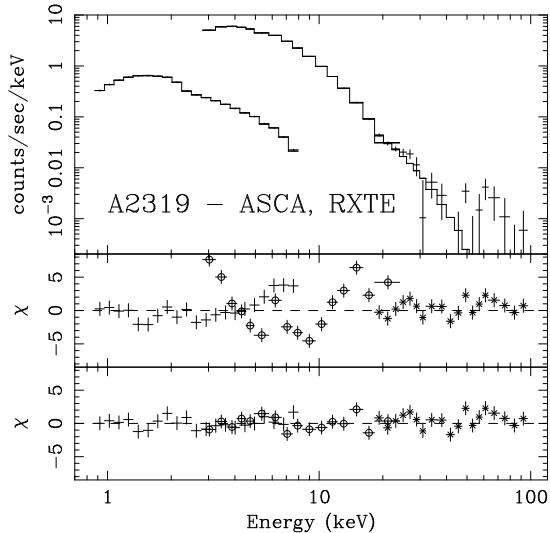


Fig. 2.— Joint fit to ASCA and RXTE data with a common Raymond-Smith thermal model and an RXTE-only power-law component. The displayed data points have been combined from adjacent energy channels of the two ASCA GIS detectors, two RXTE PCA detectors (circles) and the two RXTE HEXTE clusters (crosses). The upper panel shows the data and best fit, the middle panel shows large residuals to the best isothermal fit, and the bottom panel shows acceptable residuals after a power law component is added for the RXTE data.

unchanged at 10.1 keV, and 0.23, respectively. Fitting the second component with a power-law model changes the results mildly, with kT raised from 8.9 to 9.2 keV, $Z_{Fe} \simeq 0.29$ instead of 0.27, and a power-law index of 2.5 rather than 2.4. Errors are only slightly reduced from their respective RXTE-only values. 90% confidence upper limits of 25% were obtained to the fraction of the RXTE secondary component – power-law or thermal – that could be present in the ASCA data.

4. Discussion

The above spectral analysis of the RXTE measurements of A2319 shows clearly that the emis-

sion at ($\epsilon > 3$ keV) cannot be adequately described in terms of a single isothermal gas component. A second component is not required to fit the archival ASCA data. Above all this reflects the fact that the detection of a second component in cluster spectra is still a challenging task. Because of the much longer exposure of the RXTE observation, and the much wider spectral range of PCA and HEXTE, and given the substantial systematic uncertainties associated with the analysis of joint datasets from two satellites, we consider the spectral results of the RXTE analysis to be more robust. However, the much larger RXTE field of view, and its lack of spatial resolution, constitute sufficient ground for treating our main result as tentative, requiring independent confirmation by an X-ray satellite with the requisite wide spectral response and spatial resolution of at least $\sim 10'$. In the rest of this section we consider some of the implications of the results from the RXTE data analysis.

The measured RXTE spectrum can be well fit either by a two-temperature plasma, or by a sum of isothermal and power-law emissions. Essentially the same results were obtained in our analysis of the ~ 90 ks RXTE observation of the Coma cluster (RGB). The secondary emission component in Coma was found to contribute only $\sim 8\%$ of the total 2-10 keV emission; in A2319, this contribution is significantly higher – $\sim 15\%$ for a thermal, and $\sim 22\%$ for a power-law, secondary components.

The characterization of the thermal state of IC gas over a large (several Mpc) region by a single isothermal distribution is clearly simplistic, so it is not surprising that detailed, high quality observations with previous (*e.g.*, Markevitch 1996, Honda *et al.* 1996) and current X-ray satellites, indicate the need for more realistic spectral modeling. What is currently feasible is the measurement of appreciable emission with spectral properties sufficiently different from those of the primary thermal component with which the emission has been hitherto identified. Thus, non-

Table 1: Results of the spectral analysis

Dataset	Parameter	Isothermal	Two-Temperature	Isothermal + Power-law
RXTE	kT_1	8.6 ± 0.1	10.1 ± 0.6	8.9 ± 0.6
	Normalization ^a	0.171 ± 0.002	0.138 ± 0.025	0.129 ± 0.010
	kT_2 (keV)		2.8 ± 0.6	
	Normalization ^a		0.059 ± 0.010	
	$f(2-10 \text{ keV})$ ($\text{erg cm}^{-2} \text{ s}^{-1}$)		$(1.10 \pm 0.27) \times 10^{-4}$	
	Photon index			2.4 ± 0.3
	Fe abundance ^b	0.16 ± 0.02	0.23 ± 0.03	0.27 ± 0.041
	χ^2/dof	216/31	34/29	34/29
RXTE+ASCA	kT_1	8.6 ± 0.1	10.1 ± 0.7	9.2 ± 0.5
	Normalization ^a	0.172 ± 0.002	0.140 ± 0.014	0.127 ± 0.012
	kT_2 (keV)		2.4 ± 1.0	
	Normalization ^a		0.061 ± 0.010	
	$f(2-10 \text{ keV})$ ($\text{erg cm}^{-2} \text{ s}^{-1}$)			$(4.0 \pm 1.0) \times 10^{-11}$
	Photon index			2.5 ± 0.3
	Fe abundance ^b	0.16 ± 0.02	0.23 ± 0.03	0.29 ± 0.04
	χ^2/dof	313/50	49/48	50/48

Notes:

All quoted errors are at the 90% confidence level.

^ae.m. = Raymond-Smith emission measure in units of $10^{-14} \int N_e N_H dV / 4\pi D^2$, where D is the luminosity distance and N_e , N_H are the total number of electrons and protons, respectively.

^bAbundance is expressed relative to solar values.

isothermality of IC gas can be characterized in first order by a second thermal component with a temperature different from the main component. Alternatively, a secondary component could have a power-law form, associated with emission from a nonthermal distribution of energetic electrons in either powerful radio sources (and other active galaxies), or in extended regions of the IC space. The best-fit analysis presented above confirms the likelihood of both these two spectral possibilities, which - from a formal statistical point of view - have been found to be both likely. Let us first consider some of the physical implications from the possible presence of each of these spectral components. It may be considered natural to expect that a second emission component is also thermal, and that this is just a realistically testable manifestation of what is actually a continuous temperature distribution in the IC gas. This by itself is almost self-evident; what may be unclear, however, is whether $\sim 15\%$ of the deduced 2-10 keV flux from $kT_2 \sim 2 - 3$ keV gas is physically likely, and whether such emission is consistent with previous measurements which could have probed it.

There is at best only some indication for a temperature gradient in the central region of A2319. An average temperature, $kT \simeq 10.0 \pm 0.7$ keV, was determined from ASCA measurements (Markevitch 1996) of the central $\sim 15'$ radial region. In most of this region the temperature was found to be closer to 11 keV, whereas a lower ($kT \simeq 8.4 \pm 1.2$ keV) value was measured within a subcluster area. BeppoSAX/MECS measurements lead to a similar value of $kT \simeq 9.6 \pm 0.3$ keV for the mean temperature in roughly the same region; no evidence is seen in these data for a significant decrease in the temperature. However, the effective radius of the RXTE FOV is about twice the size of the region probed by the ASCA and MECS measurements, so a large-scale temperature gradient is perhaps even more likely to be detected by the RXTE. It is of interest, therefore, to determine the temperature profile

that is consistent with our results, and we did so in the context of polytropic gas models, adopting the approach developed by RGB in their similar analysis of RXTE measurements of the Coma cluster. As in the case of the latter cluster, no acceptable combination of the relevant parameter values (polytropic index and the density profile β parameter) is found to yield values of the temperatures and fluxes which are consistent with the results of the observations. Invariably, very high central temperatures are required in order to have substantial low temperature emission in the outer region of the cluster. This is in direct conflict with the results obtained from the high spatial resolution ROSAT, ASCA, and BeppoSAX/MECS measurements cited above. The inconsistency of polytropic temperature profiles with the ROSAT results was previously noted also by Trevese, Cirimele, & Simone (2000).

Can the two spectral components be explained as emission from lower temperature gas clumps surrounded by hotter diffuse gas? The possibility that IC gas may be appreciably clumped, to the extent that its emission characteristics differ in a measurable way from those of uniformly distributed gas, was previously investigated in the context of an isobaric equilibrium model for the two components. Various considerations lead to the conclusion (e.g., Rephaeli & Wandel 1984, Holzapfel *et al.* 1997) that only a very small fraction of the gas can survive in small clumps over relevant cluster timescales ($> 10^9$ yr). This fraction is too small to account for nearly 15% of the total flux from the clouds. We therefore conclude that even though IC gas may not be fully isothermal, the deduced level of additional low-temperature emission required to fit the RXTE data is considerably higher than can be readily explained by either polytropic, or clumpy gas distributions.

The possibility that the additional spectral component is nonthermal was found to be statistically about equally likely, as quantified in the previous section. Consider now the physi-

cal implications from the substantial power-law component that we have deduced. We first note that there is one known AGN, RXJ1923.1+4341, at a projected distance of 34' from the center of A2319, which was observed in surveys by both the *Einstein* and ROSAT satellites. The measured (IPC and PSPC) fluxes differ by at most a factor of 2, but are at least a factor ~ 60 lower than the flux deduced here in the second component of A2319. It is therefore unlikely that the emission is from bright sources in the RXTE field of view. The fact that no temporal variability is seen in our data provides additional evidence for no appreciable AGN contribution, but does not, of course, rule it out.

An eminently reasonable possibility is that the nonthermal emission results from Compton scattering of the radio-producing electrons by the CMB. Diffuse radio emission from A2319 was measured at 26 and 610 MHz (Erickson, Mathews, & Viner 1978; Harris & Miley 1978) from a central 20' region. Feretti, Giovanini, & Böhringer (1997) have recently reported the results of WSRT and VLA observations at 323, 327, 1420, and 1465 MHz. The emission is found to be more extended than previously determined (and also more powerful than that in the Coma cluster). Properties of the emission vary considerably across the radio emitting region, particularly the spectral index, for which the range $\sim 0.9 - 2.2$ was deduced (Feretti *et al.* 1997; see also Molendi *et al.* 1999). Diffuse IC emission is expected to have a steeper spectrum than in galaxies (whose indices are typically in the rough range $\sim 0.7 - 0.8$) due to continued aging resulting from Compton-synchrotron losses over (long) propagation times to the IC space. This index is thus predicted to be steeper by $\sim 1/2$, as has been found to be the case in the Coma cluster. (A lower measured value might indicate incomplete subtraction of galactic emission.) The measured radio index is thus quite uncertain, but can roughly be taken as 1.5 ± 0.6 . Perhaps a more useful characterization of the spectrum is its flux

level of 1.45 Jy at 408 MHz (Feretti *et al.* 1997).

Radio measurements imply the presence of electrons with energies of at least few GeV. Compton scattering of the electrons by the CMB boosts photon energies to $\sim 1 - 100$ keV, and probably even higher. The spectral (photon) flux depends strongly on the value of the mean, volume-averaged magnetic field, B . If we identify this emission as due to Compton scattering by the same electrons that give rise to the observed radio emission, then the implied radio index would be $\simeq 1.5 \pm 0.3$. With this value of the index, the deduced power-law flux, and the measured flux at 408 MHz, we can compute B , using the usual Compton-synchrotron formulae (*e.g.*, Rephaeli 1979). Doing so we estimate B to be in the range $\sim 0.1 - 0.4 \mu\text{G}$, when account is taken of the combined uncertainty intervals of the coefficient and index in the power-law X-ray flux. While the mean value of the magnetic field is independent of the source size and distance (when it is assumed that the radio and HEX sources have the same size), the relativistic electron energy density, ρ_e , does depend on these quantities, and the range of electron energies. With $B = 0.1 - 0.4 \mu\text{G}$, and integrating the electron energy distribution over energies in the observed radio and X-ray bands, we obtain $\rho_e \sim (2 - 5) \times 10^{-14} (R/(2 \text{ Mpc}))^{-3} \text{ erg cm}^{-3}$ for the mean electron energy density in a 2 Mpc spherical region at a (luminosity) distance of 341 Mpc (with

We emphasize that due to the lack of spatial information our estimates of the the mean value of the magnetic field, and especially the electron energy density, are just rough averages. In particular, we caution against drawing definite conclusions based on the disparity between the generally lower field values determined from the combination of X-ray and radio observations (Rephaeli, Gruber & Blanco 1999, Fusco-Femiano *et al.* 1999), and field values determined from Faraday rotation measurements (see, *e.g.*, Kim, Tribble & Kronberg 1991, Clarke,

Kronberg, & Böhringer 2001). For a more extensive discussion of this issue, see Goldshmidt & Rephaeli (1993), and Newman, Newman & Rephaeli (2001).

As noted in the Introduction, nonthermal emission in the observed energy range can possibly be produced also by nonthermal bremsstrahlung of suprathermal electrons (Kaastra *et al.* (1998, Sarazin & Kempner 2000). However, this interpretation requires the identification of a second energetic electron population which is distinct from the relativistic population that produces the observed radio emission. The determination of the exact properties of the energetic electron energy distribution would necessitate more accurate spectral and spatial measurements.

The flux in the nonthermal component reported here is comparable to the limit obtained from the BeppoSAX PDS measurements (Molendi *et al.* 1999); they report an upper bound (at 90%) of $\sim 2.3 \times 10^{-11} \text{ erg cm}^{-3} \text{ s}^{-1}$ on the flux in the PDS band (13-200 keV), as compared with our measured value of $\sim (2.5 \pm 0.36) \times 10^{-11} \text{ erg cm}^{-3} \text{ s}^{-1}$ (both at 90% confidence). The nonthermal X-ray luminosity (taking a luminosity distance of $\sim 341 \text{ Mpc}$) in the same band is quite substantial, $\sim (3.5 \pm 0.5) \times 10^{44} \text{ erg s}^{-1}$, when compared with the bolometric thermal luminosity, $\sim 2.5 \times 10^{45} \text{ erg s}^{-1}$.

In conclusion, deep exposure of A2319 with the RXTE satellite provides strong evidence for a second component in the spectrum of A2319. While from merely a statistical point of view there is no preference in the data for a power-law as compared to thermal secondary emission, the very low temperature deduced for the second component is both observationally and theoretically problematic, whereas nonthermal emission is expected based on radio measurements. It will be of great interest to observe A2319 with the IBIS instrument aboard the upcoming INTEGRAL satellite. The IBIS broad spectral band and imaging capabilities will provide essential information on the spatial distribution of the high-

energy emission from the cluster. This will likely lead to an unequivocal identification of the nature of the second spectral component.

The scope of the work presented in this paper was expanded by performing a joint RXTE and ASCA data analysis; we thank the referee for urging us to do so.

References

- Bowyer, S., & Berghofer, T.W. 1998, ApJ, 506, 502
- Bowyer, S., *et al.* 1999, ApJ, 526, 592
- Clarke, T.E., Kronberg, P.P., & Böhringer, H. 2001, ApJ, 547, L111
- Erickson, W.C., Matthews, T.A., & Viner, M.R. 1978, ApJ, 222, 761
- Feretti, L., *et al.* 1997, New Astron., 2, 501
- Fusco-Femiano, R. *et al.* 1999, ApJL, 513, L21
- Fusco-Femiano, R. *et al.* 2000, ApJL, 534, L7
- Giovannini, G., *et al.* 1993, ApJ, 406, 399
- Goldshmidt, O., & Rephaeli, Y., 1993, ApJ, 411, 518
- Harris, D.E., & Miley, G.K. 1978, A&A Supp., 34, 117
- Henriksen, M. 1998, ApJ, 50, 389
- Henriksen, M., *et al.* 1999, ApJ, 511, 666
- Holzappel, W.L., *et al.* 1997, ApJ, 480, 449
- Honda, H., *et al.* 1996, ApJ, 473, L71
- Irwin, J.A., Bregman, J.N., & Evrard, A.E. 1999, ApJ, 519, 518
- Kaastra, J.S. *et al.* 1998, Nuc. Phys. B, 69, 567
- Kaastra, J.S. *et al.* 2000, ApJL, 519, L119
- Kim, K.T., *et al.* 1990, ApJ, 355, 29
- Lampton, M., Margon, B., & Bowyer, S. 1976, ApJ, 208, 177
- Markevitch, M. 1996, ApJ, 465, L1
- Molendi, S., *et al.* 1999, ApJ, 525, L73
- Newman, W.I., Newman, A.L., & Rephaeli, Y. 2001, preprint
- Wilms, J., *et al.*, 1999, ApJ, 522, 460
- Rephaeli, Y. 1979, ApJ, 227, 364

- Rephaeli, Y., Gruber, D.E., & Rothschild, R.E. 1987, *ApJ*, 320, 139
- Rephaeli, Y., & Gruber, D.E. 1988, *ApJ*, 333, 133
- Rephaeli, Y., Gruber, D.E., & Blanco, P.R. 1999, *ApJ*, 511, L21
- Rephaeli, Y., & Silk, J. 1995, *ApJ*, 442, 91
- Rephaeli, Y., Ulmer, M., & Gruber, D.E. 1994, *ApJ*, 429, 554
- Rephaeli, Y., & Wandel, A. 1984, *MNRAS*, 215, 453
- Sarazin, C.L., & Kempner, J.C. 2000, *ApJ*, 533, 73
- Sarazin, C.L., & Lieu, R. 1998, *ApJ*, 494, L177
- Valinia, A. *et al.* 1999, *ApJ*, 515, 42